ACS OMEGA

Article

Cite This: ACS Omega 2019, 4, 22048−22056

http://pubs.acs.org/journal/acsodf

New ^{99m}Tc-Labeled Digitoxigenin Derivative for Cancer Cell Identification

Jennifer Munkert,*[,†] Eliza R. Gomes,[‡] Lucas L. Marostica,[∥] Betânia B. Cota,[⊥] Cristina L. M. Lopes,[‡] Saulo F. Andrade,[#] José D. de Souza Filho,[§] Ricardo J. Alves,[‡] Monica C. Oliveira,[‡] Fernão C. Braga,[‡] Cláudia M. O. Simões,[∥] Rodrigo M. Pádua,*[,‡] and André L. B. de Barros[‡]

[†]Department of Biology, Friedrich-Alexander-Universität Erlangen-Nürnberg, Staudtstrasse 5, 91058 Erlangen, Germany

[‡]Faculty of Pharmacy and [§]Department of Chemistry, Universidade Federal de Minas Gerais, Av. Pres. Antônio Carlos, 6627, Belo Horizonte, MG 31270-901, Brazil

[∥]Department of Pharmaceutical Sciences, Universidade Federal de Santa Catarina, Florianópolis, SC 88040-970, Brazil

[⊥]Laboratório de Química de Produtos Naturais Bioativos, Centro de Pesquisa René Rachou, Fundação Oswaldo Cruz, Av. Augusto de Lima, 1715, Belo Horizonte, MG 30190-002, Brazil

[#]Faculty of Pharmaceutical Sciences, Universidade Federal de Rio Grande do Sul, Av. Ipiranga, 2752, Porto Alegre, RS 90610-000, Brazil

Supporting Information

ABSTRACT: In recent years, cardiac glycosides (CGs) have been investigated as potential antiviral and anticancer drugs. Digitoxigenin (DIG) and other CGs have been shown to bind and inhibit Na^+/K^+-adenosinetriphosphatase (ATPase). Tumor cells show a higher expression rate of the Na^+/K^+-ATPase protein or a stronger affinity towards the binding of CGs and are therefore more prone to CGs than non-tumor cells. Cancer imaging techniques using radiotracers targeted at specific receptors have yielded successful results. Technetium-99m (^{99m}Tc) is one of the radionuclides of choice to radiolabel pharmaceuticals because of its favorable physical and chemical properties along with reasonable costs. Herein, we describe a new Na^+/K^+-ATPase targeting radiotracer consisting of digitoxigenin and diethylenetriaminepentaacetic acid (DTPA), a bifunctional chelating ligand used to prepare ^{99m}Tc-labeled complexes, and its evaluation as an imaging probe. We report the synthesis and characterization of the radiolabeled compound including stability tests, blood clearance, and biodistribution in healthy mice. Additionally, we investigated the binding of the compound to A549 human non-small-cell lung cancer cells and the inhibition of the Na^+/K^+-ATPase by the labeled compound in vitro. The ^{99m}Tc-labeled DTPA−digitoxigenin (^{99m}Tc-DTPA−DIG) compound displayed high stability in vitro and in vivo, a fast renal excretion, and a specific binding towards A549 cancer cells in comparison to non-tumor cells. Therefore, ^{99m}Tc-DTPA−DIG could potentially be used for non-invasive visualization of tumor lesions by means of scintigraphic imaging.

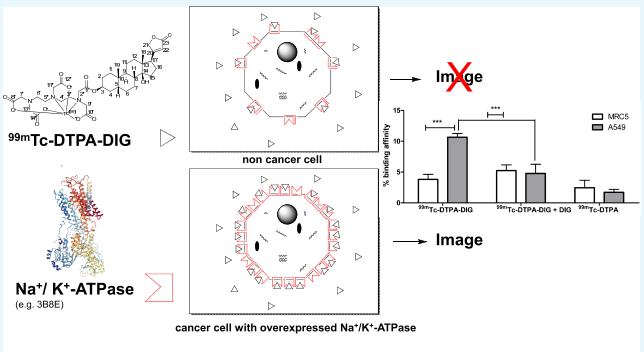

INTRODUCTION

Lung cancer is considered to be one of the most aggressive tumors with a very low survival rate; therefore, patients would benefit from early diagnosis and treatment.[1] Nuclear medicine and radionuclides are valid strategies for early cancer detection since they detect physiological changes in the target tissue. Other imaging methods, such as ultrasound, computed tomography, and magnetic resonance imaging, are especially able to identify morphological changes.[2]

Cardiac glycosides (CGs), including cardenolides, are natural products used for treating cardiac insufficiency in humans, as they bind to and inhibit Na^+/K^+-adenosinetriphosphatase (ATPase) in the myocardium, resulting in an increased cardiac output by enhancing the force of contraction. The Na^+/K^+-ATPase is a ubiquitously expressed P-type heteromeric integral membrane protein complex of eukaryotic cells, which actively transports three sodium and two potassium ions across the cell membrane using adenosine 5′-triphosphate (ATP) hydrolysis as the driving force.[3,4] It consists of three subunits—a catalytic α subunit, a stabilizing and activity-modulating β subunit, and a regulatory γ subunit, also known as an auxiliary FXYD2 protein.[4,5]

Received: September 26, 2019
Accepted: November 14, 2019
Published: December 11, 2019

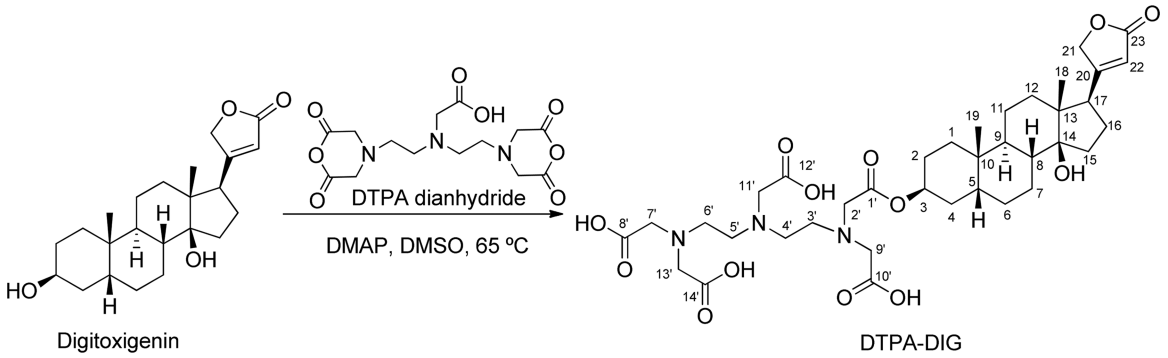

Figure 1. Chemical synthesis of DTPA−DIG. DIG (0.29 mmol) was used as a substrate, DMSO was used as a solvent, and DMAP (0.22 mmol) was added as a catalyst. The reaction was stirred under calcium chloride protection for 8 h at 65 °C.

Mutations and altered expression of Na^+/K^+-ATPase(s) have been linked to several diseases, like Alzheimer's disease, diabetes mellitus, or the growth of cancer cells. Cancer-promoting effects seem to correspond with mutations and differences in expression rates of the α- and β-subunits of the Na^+/K^+-ATPase.[6] Different relative expressions of Na^+/K^+-ATPase subunits further influence the susceptibility and binding affinity to specific cardenolides.[4] Lately based on the before-mentioned results, new therapeutic applications, besides the use of cardenolides to treat congestive heart failure, for various other diseases, e.g., viral infection or ischemic stroke, have been described.[7,8] Recent studies have further reported an increased susceptibility of cancer cells to cardenolides (reviewed in refs 9−11) and their antiviral activity.[7,12,13] It has been shown that several cancer cell lines, including the A549 non-small-cell lung cancer cell line, overexpress Na^+/K^+-ATPase proteins on their membrane, especially the α-subunit, on which cardenolides like digitoxigenin (DIG) bind with high affinity.[11,14,15] For that reason, radiolabeled DIG may be an interesting probe to identify and localize tumors or even to monitor tumor extent.

Technetium-99m (^{99m}Tc) has often been used to label radiopharmaceuticals, due to its suitable physical and chemical properties, along with reasonable radionuclide cost.[16] Several chelating agents are currently used to prepare stable complexes with ^{99m}Tc, including diethylenetriaminepentaacetic acid (DTPA), which requires mild labeling conditions and fast reaction rates at room temperature. This is an important characteristic of thermosensitive compounds since they may be degraded during the labeling process.

The purpose of this study was the evaluation of the new compound ^{99m}Tc-DTPA−digitoxigenin (^{99m}Tc-DTPA−DIG) as a tumor-targeting probe. To achieve this aim, DTPA−digitoxigenin (DTPA−DIG) was synthesized and characterized by Fourier transform infrared (FTIR), NMR, and mass spectrometry (MS). Subsequently, the radiolabeling efficiency and stability were examined, and in vitro cell binding in the A549 lung cancer cell line compared to the MRC-5 non-tumor cell line was studied. Additionally, biodistribution was monitored and scintigraphic images were taken in healthy mice to estimate the pharmacokinetics of the new probe.

RESULTS AND DISCUSSION

Synthesis and Structural Analysis of DTPA−DIG. The reaction was carried out in different solvents ranking from dimethyl sulfoxide (DMSO) to pyridine and tetrahydrofuran, to improve the product yield (Table S1). Product formation was only observed in DMSO due to the good solubility of the educts in this solvent (Figure 1). The isolation of the product DTPA−DIG from the reaction medium was challenging, since it has four free carboxyl groups and an ester linkage prone to hydrolysis at either high or low pH values. DTPA−DIG was isolated and purified by preparative reversed-phase high-performance liquid chromatography (RP-HPLC) employing mild conditions (Figure S1). Fractions containing the product were pooled, and acetonitrile (ACN) was removed by evaporation under reduced pressure. In the sequence, the residual water was eliminated by lyophilization to afford DTPA−DIG as a white amorphous solid (61% yield on molar base). The infrared spectrum of DTPA−DIG showed a carboxylic acid O−H stretch at 3200−2500 cm^{-1}; an alkyl C−H stretch at 2936−2860 cm^{-1}; C═O stretches at 1712, 1778, and 1733 cm^{-1}, respectively, of carboxylic acid, lactone and ester as well as a C−O strong stretch at 1213 cm^{-1}. This last band demonstrates the presence of an ester linkage in DTPA−DIG (Figure S2). MS spectra were acquired for the protonated molecular ion MH^+ at m/z 750.6 compatible with the chemical formula of $C_{37}H_{55}N_3O_{13}$ from the monoester DTPA−DIG (Figure S3). The ^{1}H NMR spectrum of DTPA−DIG showed the methylene protons of the DTPA group at the interval δ 2.82−3.63 and all protons of the aglycone digitoxigenin (Figures 1 and S4, and Table 1). The assignment of the resonance signals was confirmed by data from the heteronuclear single quantum coherence (HSQC) spectrum. Two doublets centered at δ 4.98 and 4.88 (d, $J_{21a,21b}$ = 17.5 Hz) were ascribed to the geminal coupling of the methylene protons at C-21. The C-3 methine proton resonates at δ 5.03, a downfield shifted-value in comparison to H3α of the free aglycone, due to the ester linkage with the DTPA group (Figures S4 and S5a,b). The HSQC spectrum was very useful to determine the ^{1}H/^{13}C one-bond shift correlations of all hydrogen-bearing carbon atoms in DTPA−DIG. Complete ^{1}H/^{13}C one-bond shift correlations of all protonated carbon atoms are presented in Table 1 (Figure S5a,b). The ^{1}H−^{1}H correlated spectroscopy (COSY) spectrum was useful for assigning the hydrogen resonances of DTPA−DIG (Figure S6a−c). The C-3 methine proton (δ 5.03) showed cross-peaks with the methylene hydrogens linked to C-2 (δ 1.50 and 1.61) and C-4 (δ 1.33 and 1.94), whereas the C-17 methine proton (δ 2.73) exhibited correlation spots with C-16 methylene protons (δ 2.05 and 1.81) (Figure S6). The ^{13}C NMR spectrum of DTPA−DIG showed the resonance signals of 37 atoms (Table 1 and Figure S7), which were identified as two methyl, nineteen methylene, and six methine carbon atoms by

DOI: 10.1021/acsomega.9b03167
ACS Omega 2019, 4, 22048−22056

Table 1. ^{1}H and ^{13}C Chemical Shifts (ppm) for DTPA−DIG (400 MHz for ^{1}H and 100 MHz for ^{13}C; DMSO-d_6)

carbon/hydrogen		^{1}H (J in Hz)	^{13}C
1	α	1.24	30.3
	β	1.51	
2	α	1.50	24.4[a]
	β	1.61	
3	α	5.03 brs	70.5
4	α	1.94	29.9
	β	1.33	
5	β	1.59	36.7
6	α	1.19	26.4[a]
	β	1.75	
7	α	1.77	20.8[b]
	β	1.12	
8	β	1.48	40.9
9	α	1.64	34.7
10			34.8
11	α	1.35	20.9[b]
	β	1.15	
12	α	1.38	38.9
	β	1.38	
13			49.4
14	(β-OH)	83.7	
15	α	2.08	32.2
	β	1.63	
16	α	2.05 ($J_{16\alpha,17\alpha}$ = 5.0 Hz)	26.1
	β	1.81 ($J_{16\beta,17\alpha}$ = 9.8 Hz)	
17	α	2.73 (dd $J_{17\alpha,16\beta}$ = 9.8 Hz)	50.2
18		0.78 s	15.7
19		0.90 s	23.5
20			176.3
21	a	4.98 (d J^{a} = 17.5 Hz)	73.1
	b	4.88 (d J^{b} = 17.5 Hz)	
22		5.91 s	116.2
23			173.8
1′			170.4
2′		3.53 brs	55.0
3′		2.89 brs	50.2
4′		2.89 brs	50.2
5′		3.00 brs	51.8
6′		3.00 brs	55.8
7′		3.44 brs	55.0
8′			172.5
9′		3.44 brs	55.0
10′			172.5
11′		3.58 brs	55.0
12′			169.6
13′		3.44 brs	55.0
14′			172.5

[a]Values may be interchangeable. [b]Values may be interchangeable. s, singlet; brs, broad singlet; dd, doublet of doublets.

the distortionless enhancement by polarization transfer (DEPT)-135 experiment (Figure S8), along with ten quaternary carbons. The signals at δ 176.3 and 174.0 were ascribed, respectively, to C-20 and C-23 of the α,β-unsaturated lactone ring. The carbonyls at C-8′, C-10′, and C-14′ resonate with the same chemical shift value, at δ 172.5, while the signals at δ 170.4 and 169.8 were ascribed to C1′ and C-12′ carbonyls (DTPA group), respectively. The downfield chemical shift values of C-3, C-14, and C-21 were due to the presence of geminal oxygen functionalities on these carbon atoms. The heteronuclear multiple bond correlation (HMBC) experiment was useful for the assignments presented in Table 1 (Figure S9a−f). Nuclear Overhauser enhancement spectroscopy (NOESY) data, coupling constants, and comparison with literature records[17] were used to distinguish the diastereotopic protons within the methylene groups, which exhibited characteristic patterns for axially or equatorially located hydrogens (Table 1). Hence, NOESY depicted spatial interactions between the C-3 methine proton (δ 5.03) and C-2′ methylene (δ 3.53) hydrogens. These NOESY observations indicated that C-3 oxygen was bonded to C-1′ through an ester linkage (Figure S10a−c). The presence of a single ester bond in the compound DTPA−DIG was also supported by ^{1}H, ^{13}C, mass spectral, and infrared data,[17] as discussed above.

^{99m}Tc Labeling of DTPA−DIG, Radiochemical Purity, and in Vitro Stability. DTPA−DIG was radiolabeled with ^{99m}Tc in the presence of stannous chloride ($SnCl_2$) as a reducing agent. To evaluate the effect of the reducing agent on the labeling process, three different amounts of the reagent (200, 270, 330 μg) were tested, and the radiochemical purities were determined.

Thin-layer chromatography (TLC) over silica gel was used to determine the radiochemical yield of the ^{99m}Tc-DTPA−DIG, employing two distinct eluent systems (acetone or glacial acetic acid/water 15:85, v/v). The radiolabeling reaction can yield $^{99m}TcO_4^-$ and $^{99m}TcO_2$. $^{99m}TcO_4^-$ migrated with the solvent front in both TLC systems, glacial acetic acid/water (15:85, v/v) and acetone (R_f = 0.9−1.0), whereas the radiocolloids ($^{99m}TcO_2$) remained immobilized at the point of application in both solvents (R_f = 0.0). ^{99m}Tc-DTPA−DIG showed R_f values of 0.9 or 0.0 in glacial acetic acid/water (15:85, v/v) or in acetone as eluents. High radiochemical yields play a crucial role in radiopharmaceutical applications since the presence of radiochemical impurities has to be limited as they cause images of low quality and they might also accumulate in the thyroid and stomach as well as in the liver and spleen.[2] Ideally, radiopharmaceuticals should be at least 90% pure, in terms of radioactivity species.[18] The use of 200 μg of stannous chloride in the labeling reaction afforded a suitable overall radiolabeling yield (95.8 ± 2.2%), whereas amounts of 270 and 330 μg led to a product with insufficient purity (68.7 ± 7.2 and 77.1 ± 6.6%, respectively). The success of radiolabeled DTPA−DIG was further evidenced by ultra-performance liquid chromatography (UPLC)/MS analysis, where the ^{99m}Tc-labeled compound gave signals in the negative ion mode at m/z 820 [^{99m}Tc-DTPA−DIG − CO_2 + H_2O − H]$^-$, m/z 864 [^{99m}Tc-DTPA−DIG + H_2O − H]$^-$, and m/z 883 [^{99m}Tc-DTPA−DIG + $2H_2O$ − H]$^-$ (Figure S11).

The stability of the labeled conjugate is also pivotal for the successful application of a radiopharmaceutical.[19] Aiming for an in vivo administration of ^{99m}Tc-DTPA−DIG, its radiochemical stability was evaluated using the two distinct solvent systems (acetone or glacial acetic acid/water 15:85, v/v) mentioned above at 1, 2, 4, 8, and 24 h in the presence of NaCl 0.9% (w/v) solution at room temperature (23 °C) or in the presence of plasma at 37 °C, under agitation. In both conditions, the product including the ester bond remained stable within the evaluated interval (Figure 2). If the isotope chelation of radiodiagnostic agents does not remain stable for several hours, the biodistribution and imaging data will be unreliable.[20]

DOI: 10.1021/acsomega.9b03167
ACS Omega 2019, 4, 22048−22056

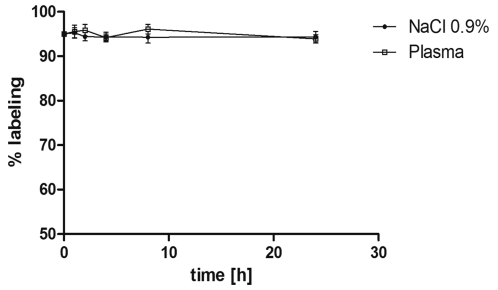

Figure 2. Radiochemical stability of ^{99m}Tc-DTPA−DIG in saline (0.9% NaCl) at room temperature (23 °C) and plasma at 37 °C. Radiochemical stability was tested up to 24 h (n = 6).

Inhibition of Na^+/K^+-ATPase Activity by ^{99m}Tc-DTPA−DIG and Specific Binding of ^{99m}Tc-DTPA−DIG towards MRC-5 and A549 Cells. In a first step, the inhibition rate of ^{99m}Tc-DTPA−DIG against Na^+/K^+-ATPase activity (mixture of α1,2,3 subunit from the porcine cortex) was evaluated at 0.1 μM, a concentration corresponding to the IC_{50} value of the labeled compound against A549 cells (IC_{50} A549 cell line: 0.12 μM; IC_{50} non-tumor MRC-5 cell line: 0.78 μM; Figure S12). Inhibition of porcine Na^+/K^+-ATPase (α1,2,3 subunit) was investigated to assay the effect of the labeling solution, free DTPA, and the labeling of DTPA−DIG on the Na^+/K^+-ATPase activity in general (Figure 3). The obtained data

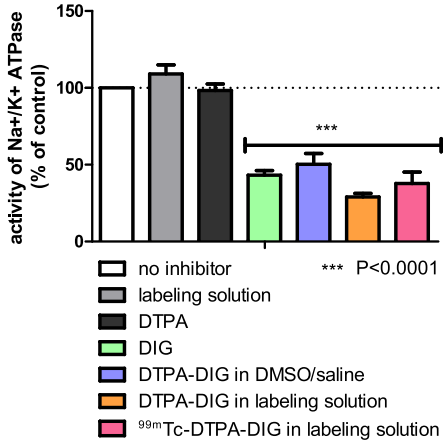

Figure 3. Inhibition of Na^+/K^+-ATPase activity by DIG, DTPA, DTPA−DIG, and ^{99m}Tc-DTPA−DIG tested at 0.1 μM. Effects of DIG, DTPA−DIG, and ^{99m}Tc-DTPA−DIG on Na^+/K^+-ATPase activity were assayed with the Na^+/K^+-ATPase α1,2,3 subunit of the porcine cortex. Results indicated Na^+/K^+-ATPase inhibition by DIG, DTPA−DIG, and ^{99m}Tc-DTPA−DIG. However, labeling solution, as well as DTPA alone, has no influence on the activity of Na^+/K^+-ATPase.

showed that neither the reagents in the labeling solution nor DTPA alone has any effect on Na^+/K^+-ATPase activity. However, concentrations of 0.1 μM of DIG, DTPA−DIG, and ^{99m}Tc-DTPA−DIG reduced the enzymatic activity to less than 50%. This indicated that neither DTPA nor ^{99m}Tc interfered with the binding of DIG to the Na^+/K^+-ATPase α subunit and that the interaction between the cardenolide derivative and its target structure remains intact. This is an important and positive result for assessing the suitability of the radiolabeled compound as a potential imaging probe.

Cancer drug development is currently focused on the search of specific biochemical differences between malignant and normal cells, a strategy that is also adopted in the development of diagnostic tools for the identification of tumor cells. Na^+/K^+-ATPase is known to be the target receptor for CGs.[21] This ubiquitous enzyme belongs to the P-type ATPase family and is involved as an integral membrane protein in transporting sodium ions out of the cell and potassium ions into the cell, thus helping regulate the electrochemical gradient across the plasma membrane.[22] Human Na^+/K^+-ATPase is composed of four different isoforms of the α-subunit, acting as the catalytic subunit of the Na^+/K^+-ATPase complex (α1, α2, α3, and α4). Additionally, three different β-subunit isoforms and seven γ-subunit isoforms result in great protein viability.[23] The overall expression pattern of the Na^+/K^+-ATPase is a possible biomarker for cancer, as a high expression level of the α-subunit and a low expression of the β-subunit may indicate an increased risk for cancer.[6] Keeping in mind that Na^+/K^+-ATPase is a specific target for CGs and the different expression rates of its subunits in malignant to non-malignant cells, the protein constitutes a potential target to identify tumors or to monitor tumor mass and growth.

Cardiac glycosides including cardenolides and their derivatives are known to bind to the α-subunit of the Na^+/K^+-ATPase, impairing the attachment of ATP and thus disrupting the effect of the enzyme.[24] Depending on the concentration and structure of CGs, either the Na^+/K^+-ATPase can be inhibited or the Na^+/K^+-ATPase signalosome can be activated, both inhibiting cell proliferation and impeding cell survival.[6,25] An overexpression of the α1 subunit of the Na^+/K^+-ATPase was observed in human non-small-cell lung cancer A549 cell lines.[26] The authors demonstrated[26] that A549 cells, overexpressing the α1 subunit of the Na^+/K^+ ATPase, are more susceptible to selected cardiac glycosides, such as digoxin, ouabain, and the hemisynthetic derivative of 2″-oxovoruscharin (UNBS1450). The specific binding of cardenolides to the overexpressed α1 subunit of A549 cells is a promising and unique feature that led us to select this cell line for an in vitro binding study.

Therefore, the specific binding of ^{99m}Tc-DTPA−DIG to the human non-small-cell lung cancer A549 cell line versus the non-tumor human fetal lung fibroblast MRC-5 cell line was evaluated by quantifying the overall radioactivity level. The concentration of 0.1 μM was also used for examining the cellular binding of ^{99m}Tc-DTPA−DIG to the A549 cancer cells and the non-tumor human fetal lung fibroblast MRC-5 cells. The in vitro results showed a significantly higher binding of ^{99m}Tc-DTPA−DIG to A549 cells than to non-tumor MRC-5 cells. ^{99m}Tc-DTPA−DIG binding to A549 cells was reduced to the rate of non-tumor MRC-5 cells when it was co-incubated with a 10-fold excess of free digitoxigenin (Figure 4).

The outcomes from these experiments, i.e., the high specific binding of ^{99m}Tc-DTPA−DIG to A549 cancer cells, low affinity of ^{99m}Tc-DTPA to A549 cancer cells, and the inhibition of the Na^+/K^+-ATPase by ^{99m}Tc-DTPA−DIG, let us conclude that the higher specificity of DIG for the lung cancer cell line A549 results from an increase in the expression of the Na^+/K^+-ATPase. The selectivity of DIG towards the A549 cell line compared with other cancer cell lines has been previously described in cytotoxicity studies.[27,28] A higher expression of the Na^+/K^+-ATPase α1 subunit was reported for A549 cell lines.[26] . In the same direction, an increased expression of certain subunits of Na^+/K^+-ATPase was found in bladder and

DOI: 10.1021/acsomega.9b03167
ACS Omega 2019, 4, 22048−22056

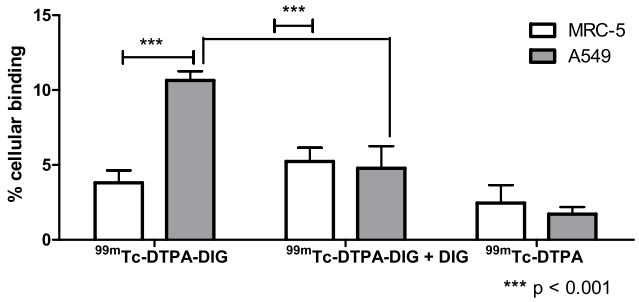

Figure 4. Binding of ^{99m}Tc-DTPA−DIG to MRC-5 non-tumor lung cell lines and to A549 lung cancer cell lines after 2 h of incubation. ^{99m}Tc-DTPA−DIG showed significantly higher affinity to A549 lung cancer cell lines. Specific binding was significantly reduced by 10-fold blocking with free DIG. Results are expressed as a mean ± standard error (n = 3).

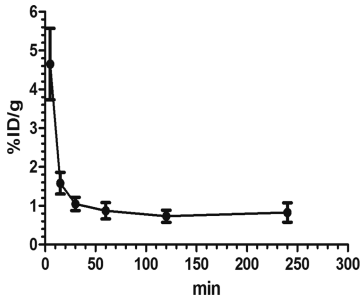

Figure 5. Blood clearance of ^{99m}Tc-DTPA−DIG in healthy mice (n = 6).

gastric cancer cells.[29,30] An alteration in the overall Na^+/K^+-ATPase activity was further described in renal carcinoma cells[4] along with an increased expression of the α1 subunit of Na^+/K^+-ATPase in the majority of glioblastomas, in comparison to normal brain cells.[31] In light of this higher expression rate of the Na^+/K^+-ATPase and the specific binding of cardenolides to their α subunit, developing imaging probes that are based on the cardenolide structure seems to be a promising strategy for tumor identification. Therefore, investigating the specific binding of ^{99m}Tc-DTPA−DIG or ^{99m}Tc-DTPA coupled to different cardenolides or cardenolide derivatives towards various cancer cell lines can be a valid and prospective strategy to evaluate their potential for tumor diagnosis. However, in a first step for gaining more information on this newly synthesized and labeled compound ^{99m}Tc-DTPA−DIG and its suitability as an imaging probe, biodistribution as well as blood clearance has to be studied in healthy mice.

Blood Clearance, Biodistribution, and Scintigraphic Images in Healthy Mice. The radiolabeled complex showed rapid blood clearance, with only 0.51 %ID/g at 0.5 h and a further decrease at 2 h (Table 2). Its half-life was 11.7 min (Figure 5).

Table 2. Biodistribution of ^{99m}Tc-DTPA−Digitoxigenin in Healthy Mice Expressed as a Mean Percentage (n = 6) of the Injected Dose/g (%ID/g) Tissue ± Standard Deviation

tissue	30 min (%ID/g)	SD	2 h (%ID/g)	SD
blood	0.51	0.08	0.43	0.16
liver	4.74	1.67	2.34	0.31
spleen	0.90	0.13	0.85	0.21
kidney	1.64	0.38	1.48	0.22
heart	0.31	0.05	0.32	0.29
lungs	1.46	0.35	0.6	0.17
thyroid	0.59	0.27	0.59	0.45
intestine	24.97	5.47	27.06	1.64
muscle	0.50	0.38	0.26	0.15

Fast blood clearance is favorable for early imaging as background radiation can lower imaging quality.[20] Biodistribution studies were conducted in healthy mice, and tissues were analyzed at 0.5 and 2 h post-injection. Maximum uptake was observed in the liver and intestine. The kidneys also showed a high uptake, suggesting that renal elimination also contributes to the radiopharmaceutical's excretion (Table 2 and Figure S13).

A relatively low uptake in the thyroid was observed, indicating high stability of the labeled complex.[32] The distribution in healthy mice was further analyzed by images. High uptake rates in the kidneys, liver and mainly in the intestine could be detected (Figure S13). Comparable low accumulation of the labeled compound in the heart of healthy mice can be due to the fact that rodents have a mutation in the α1 subunit of their Na^+/K^+-ATPase, which makes them less susceptible to CGs. For example, Ujvari and co-workers showed that as a consequence of this mutation, the Na^+/K^+-ATPase in rodents is 1000-fold more resistant to the cardenolide ouabain.[33] Additionally, cardiac α isoform expression varies depending on the species. So far, the α3 subunit, which also has a high binding affinity to CGs, has been only identified in humans, but not in rodents.[34] Therefore, the altered distribution of the isoforms in rodents might also be an explanation for the low accumulation of ^{99m}Tc-DTPA−DIG in the mice heart.

In the 1960s, the use of radiolabeled CGs made it possible to detect cardiac glycosides and their metabolites in body fluids and tissues. Studies with tritiated digoxin showed that its clearance from the human body depends on renal excretion.[35] Pharmacokinetic studies with digoxin in humans evidenced its main adsorption into the intestine, kidneys and heart and a major renal excretion.[36] Likewise, the administration of the ^{99m}Tc-labeled ouabagenin−cysteine conjugate to guinea pig, rabbit and rat also showed fast blood clearance and renal elimination. For rabbits and rats, an additional high uptake in the liver was also observed.[37] CGs aglycones like ouabagenin and digitoxigenin exhibit a reversible binding to Na^+/K^+-ATPase, whereas the binding of CGs bearing sugar moiety is irreversible and exhibits a different pharmacokinetics behavior.[38] Without sugar moieties present, the molecules dissociated in the bloodstream much faster.[36] This was further supported by the findings of ref 39, which demonstrated that ^{125}I-digoxin-iodohistamine(bis(*O*-carboxymethyloxime)) exhibits selective myocardial accumulation in guinea pigs compared with the ^{125}I-digoxigenin-iodohistamine(3-oxime) and ^{125}I-digoxigenin-iodohistamine(3-ester). Like other imaging probes already described, e.g., by de Barros and co-workers,[2] ^{99m}Tc-DTPA−DIG showed a fast blood clearance and a renal excretion. Therefore, its possible use as an imaging probe is thereby further strengthened.

CONCLUSIONS

In conclusion, the compound DTPA−DIG was successfully synthesized, characterized, and labeled with technetium-99m,

DOI: 10.1021/acsomega.9b03167
ACS Omega 2019, 4, 22048−22056

showing a high level of stability. In vitro binding assays confirmed a higher and specific affinity of ^{99m}Tc-DTPA−DIG to non-small-cell lung cancer A549 cells in comparison to human fetal lung fibroblast MRC-5 cells, probably due to the specific binding of ^{99m}Tc-DTPA−DIG to the target Na^+/K^+-ATPase. Neither the labeling solution nor DTPA inhibited significantly the Na^+/K^+-ATPase activity. ^{99m}Tc-DTPA−DIG blood levels decline fast, which allows obtaining early images. In addition, biodistribution and scintigraphic studies showed a high uptake by the intestine, liver and kidney. Taken together, the results reported here demonstrate the specificity of ^{99m}Tc-DTPA−DIG to lung cancer cells and suggest that this new radiolabeled derivative might be potentially useful for imaging techniques applied to diagnoses of tumors and other diseases that show distinct expression rates of the Na^+ /K^+-ATPase.

MATERIAL AND METHODS

Material. ^{99m}Tc was acquired from a ^{99}Mo/^{99m} Tc generator supplied by Instituto de Pesquisas Energéticas e Nucleares—IPEN (São Paulo, Brazil). Other reagents and solvents for the radiolabeling procedure were purchased from Sigma-Aldrich (São Paulo, Brazil). The human non-small-cell lung cancer A549 cell line (ATCC CCL-185) was obtained from American Type Culture Collection (ATCC, Manassas, VA). Human fetal lung fibroblast cells (MRC-5) were acquired from the European Collection of Cell Cultures (ECACC, Porton Down, WI, England). Dulbecco's modified Eagle's medium (DMEM; Gibco, Waltham, MA) was used for cell cultivation supplemented with fetal bovine serum (FBS) purchased from Sigma-Aldrich (São Paulo, Brazil). Antibiotics penicillin and streptomycin were obtained from Sigma-Aldrich (St. Louis, MO). Trypsin was acquired from Invitrogen (São Paulo, Brazil), and matrigel was obtained from Becton, Dickinson and Company-BD (Juiz de Fora, Brazil). Female BALB/c mice (15−20 g) were purchased from the central vivarium at Universidade Federal de Minas Gerais. Animals were kept under specific pathogen-free (SPF) conditions, with free access to food and water. The cages were temperature-controlled with filtered air and a regulated light−dark cycle (12:12 h). All protocols were approved by the Ethics Committee for Animal Experiments at Universidade Federal de Minas Gerais (protocol number 424/2014) and are in compliance with the guide for the care and use of laboratory animals recommended by the Institute of Laboratory Animal Resources.

Synthesis of the DTPA−DIG Compound. The reaction was performed in a preparative scale with DMSO as the solvent. First, 110 mg of digitoxigenin (0.29 mmol), 550 mg of DTPA dianhydride (1.54 mmol), and 27.5 mg of DMAP (0.22 mmol), used as the catalyst, were added to a cylindrical tube (13.5 × 3.5 cm^2). Then, 5.5 mL of DMSO was added, and the reaction mixture was heated to 65 ± 2 °C under calcium chloride protection by using a drying tube to create a water-free environment. The mixture was stirred for 8 h. Next, the reaction mixture was maintained for 48 h at 8 °C and then subjected to purification procedures.

Isolation of DTPA−DIG by Semipreparative RP-HPLC. DTPA−DIG was isolated by semipreparative RP-HPLC using a Shimadzu equipment (Shimadzu Corp., Japan) composed of wo LC6AD pumps and a manual injection valve (Rheodyne 7125, Rheodyne, CO). The injection was performed using a 1.000 μL sample loop, and detection was carried out at 200 and 220 nm, employing a dual-wavelength detector (SPD M10A) controlled by LCsolution software v.1.25 (Shimadzu Corp.). Separation was performed on an ODS column (Shim-pack PREP-ODS; 250 × 4.6 mm^2 i.d., 5 μm), using a linear gradient of 10−100% ACN with 0.1% formic acid (v/v) for elution in 20 min, at a flow rate of 7 mL/min. The obtained peak fractions were pooled, and the acetonitrile was removed in a rotary evaporator at 30 °C, followed by lyophilization to eliminate the water.

Infrared Spectroscopy. The IR spectrum was recorded on a PerkinElmer Spectrum One spectrometer (Beaconsfield, U.K.) with an attenuated total reflection (ATR) system.

NMR Analysis. ^{1}H NMR, ^{13}C NMR, DEPT-135, ^{1}H−^{1}H COSY, HSQC, HMBC, and NOESY spectra were recorded on a Bruker DRX-400 spectrometer (^{1}H 400 MHz and ^{13}C 100 MHz) in DMSO-d_6 at 300 K with tetramethylsilane (TMS) as the internal standard for both nuclei. Chemical shifts (δ) are given in ppm and J couplings in hertz (Hz).

Radiolabeling and Radiochemical Purity of DTPA−DIG with Technetium-99m. First, 1 mg of the DTPA−DIG (1.3 nmol) was dissolved in 20 μL of DMSO and diluted with 380 μL of saline. Then, 100 μL of a 1 mg/mL solution of stannous chloride (in HCl 0.25 M), as a reducing agent, was added. The pH of the solution was adjusted to 7 with a NaOH solution (140 μL of 0.1 M), and the vial was immediately vacuum-sealed. Pertechnetate ($^{99m}TcO_4^-$) was added (∼3 mCi), and the mixture was allowed to react for 15 min at room temperature (23 °C). The radiolabeling yields of the ^{99m}Tc-DTPA−DIG were determined by thin-layer chromatography (TLC) analysis on two solvent systems: acetone to determine $^{99m}TcO_4^-$ and glacial acetic acid/water (15:85) to determine $^{99m}TcO_2$. The radioactivity of centered cut TLCs was measured using an automatic scintillation counter.

An additional staining with Kedde's reagent was carried out for proving the stability of the DTPA−DIG by detection of the lactone ring after radiolabeling.

UPLC/MS Analysis of Radiolabeling. UPLC/MS analyses were carried out on an ACQUITY Ultra Performance LC system (Waters, Milford, MA) linked simultaneously to a photodiode array detector (PDA) 2996 photodiode array detector (Waters, Milford, MA) and an ACQUITY TQ Detector (Waters MS Technologies, Manchester, U.K.), equipped with a Z-spray electrospray ionization (ESI) source operating in positive and negative modes. MassLynx software (version 4.1, Waters, Milford, MA) was used to control the instruments, as well as for data acquisition and processing. Diluted sample solutions (3 μL; 0.5 mg/mL; 0.58 nmol) were injected into a reversed-phase column (BEH_{C18}, 1.7 μm, 1 × 50 mm^2, Waters, Milford, MA), which was maintained at 40 °C. The mobile phase consisted of solvent A (H_2O/0.1 HCOOH) and solvent B (acetonitrile/0.1 HCOOH) at a flow rate of 300 μL/min, eluted in a linear gradient, as follows: T = 0 min, 5% B; T = 10 min, 95% B; T = 11 min, 5% B; T = 13 min, 5% B. The effluent was introduced into a PDA detector (scanning range 210−400 nm, resolution 1.2 nm) and subsequently into an electrospray source (source block temperature 120 °C, desolvation temperature 350 °C, capillary voltage 3.5 kV, cone voltage 30 V) and nitrogen as the desolvation gas (600 L/h). Mass chromatograms were recorded in the positive and negative ionization modes.

In Vitro Stability. Radiochemical stability was evaluated in saline at room temperature and in plasma at 37 °C, under agitation, from samples taken 1, 2, 4, 8, and 24 h after incubation at room temperature (23 °C). Radiochemical

DOI: 10.1021/acsomega.9b03167
ACS Omega 2019, 4, 22048−22056

stability was determined by TLC as described above. The radioactivity was measured using an automatic scintillation counter. The number of samples per each time point was 6, and they were evaluated in duplicates.

Binding of the Radiolabeled Compound towards MRC-5 and A549 Cell Lines. *Cell Culture.* Human non-small-cell lung cancer (A549) and human fetal lung fibroblast cells (MRC-5) were cultured in DMEM supplemented with 10% (v/v) fetal bovine serum and 1% (v/v) penicillin and streptomycin as antibiotics. Cells were maintained in a humidified incubator with a 5% CO_2 atmosphere at 37 °C. The cells were grown to confluence and then harvested by trypsin dissociation. After centrifugation (500*g* for 5 min), cells were resuspended with a phosphate-buffered saline (PBS) solution (pH 7.4). Viable cells for the binding assays were quantified using trypan blue staining, and cell number was countered in a Neubauer Chamber.

Cell Viability. The colorimetric MTT assay was performed using 3-(4,5-dimethyl-1,3-thiazole-2-yl)-2,5-diphenyltetrazolium bromide (MTT). Cells (1×10^4 A549 and MRC-5 cells per well of a 96-well microtiter plate) were cultured for 48 h with various concentrations of ^{99m}Tc-DTPA−DIG. At the indicated time points, MTT was added to a final concentration of 1 mg/mL, and 200 μL of DMSO was added after 4 h of incubation at 37 °C to dissolve the formazan crystals. The absorbance was measured at 570 nm using a plate spectrophotometer (VersaMax ELISA Microplate Reader, Molecular Devices). Cells treated with 0.5% DMSO served as a negative control to define 100% viability. The percentage of viable cells was plotted against the sample concentration, and the IC_{50} values were determined based on the dose−response curves using GraphPad Prism 5.0 (GraphPad software, La Jolla, CA).

Na^+/K^+-ATPase Assay. Enzymatic activities of the Na^+/K^+-ATPase α1,2,3 subunit of the porcine cortex (Sigma) were assayed using 4 mM ATP as the substrate in a final volume of 40 μL assay buffer containing 40 mM Tris−HCl pH 7.5, 80 mM NaCl, 1 mM ethylenediaminetetraacetic acid (EDTA), and 8 mM $MgAc_2$. The negative control was assayed without enzyme, and 4 mM ATP was added after 30 min of incubation at room temperature. The positive control contained 0.05 U/mL Na^+/K^+-ATPase α1,2,3 subunits of the porcine cortex in a 30 min preincubated mixture with assay buffer; later, 4 mM ATP was added. Inhibition assays were performed by co-incubating the enzyme and individual inhibitor at concentrations of 0.1 μM for 30 min and adding 4 mM ATP solution. Reactions were stopped after 30 min of incubation, and activity was determined by measuring the Pi released according to the malachite-green test[40] Activity was scored as the percentage of reduction of absorbance subtracting the absorbance at 600 nm of the control well, relative to the positive control well. Positive control defined 100% enzyme activity. All experiments were performed in triplicates.

Binding Studies. For the binding assay, 0.1 μM of the ^{99m}Tc-DTPA−DIG, 1.3 μM of ^{99m}Tc-DTPA, and ^{99m}Tc-DTPA−DIG with excess (10-times) of free digitoxigenin were incubated at 37 °C with 250 000 viable cells/tube. This mixture was kept under agitation (140 rpm) for 120 min. Next, the material was centrifuged at 10 000 *g* for 5 min and the supernatant discarded. The pellet was resuspended in 500 μL of PBS and analyzed in an automatic scintillation counter. The experiment was performed in independent biological triplicates each consisting of three technical replicates.

In Vivo Studies in Healthy Mice. *Blood Clearance.* Aliquots of 100 μL (3.7 MBq) of the diluted ^{99m}Tc-DTPA−DIG (final volume 1800 μL) were administrated to healthy BALB/c female mice (20 g, 8 weeks old, $n = 6$, per time point) through the tail vein and blood samples were extracted 5, 15, 30, 60, 120, and 240 min after administration. Each sample was weighted, and the associated radioactivity was determined. The percentage of injected dose per milliliter of blood (%ID/mL) was determined, and the data were plotted as a function of time.

Biodistribution. Aliquots of 100 μL (3.7 MBq) of the diluted ^{99m}Tc-DTPA−DIG (final volume 1800 μL) were injected intravenously into healthy BALB/c mice (20 g, 8 weeks old, $n = 6$, six per time point). After 30 min or 2 h, mice were anesthetized (ketamine: 80 mg/kg; xylazine: 15 mg/kg) and euthanized. Blood, liver, spleen, kidney, heart, lungs, muscle, thyroid, and intestine were removed, dried on filter paper, and placed in preweighed plastic test tubes. The radioactivity was measured. A standard dosage containing the same injected amount was counted simultaneously in a separate tube, which was defined as 100% radioactivity. The results were expressed as the percentage of injected dose/g of tissue (%ID/g).

Scintigraphic Images. First, 100 μL aliquots (18 MBq) of the diluted ^{99m}Tc-DTPA−DIG (dilution to final volume 3600 μL) were injected intravenously into the tail vein of healthy BALB/c mice (20 g, 8 weeks old, $n = 6$ per time point). After 30 min, 1 h, and 2 h, mice were anesthetized (ketamine: 80 mg/kg; xylazine: 15 mg/kg) and placed horizontally under the collimator of a low-energy high-resolution γ camera (Mediso, Hungary). Images were acquired using a 256 × 256 × 16 matrix size with a 20% energy window set at 140 keV for a period of 300 s.

Statistical Analysis. All data were expressed as mean ± standard deviation of the mean. Means between the various groups were compared by one-way analysis of variance (ANOVA followed by Tukey's post hoc test). In the case of multiple comparisons, a post hoc Bonferroni correction was applied. P values <0.001 were considered statistically significant. Data were analyzed using GraphPad Prism 5 Software (GraphPad, San Diego, CA).

■ ASSOCIATED CONTENT

Supporting Information

The Supporting Information is available free of charge at https://pubs.acs.org/doi/10.1021/acsomega.9b03167.

Chemical reaction conditions, semipreparative RP-HPLC chromatogram, and infrared and MS analyses of DTPA−DIG as well as detailed NMR analysis including ^{1}H, ^{13}C, HSQC, COSY, DEPT-135, HMBC, and NOESY; MS spectrum of ^{99m}Tc-DTPA−DIG, dose−response curves of MTT assays for ^{99m}Tc-DTPA−DIG against the A549 lung cancer cell line, and non-tumor MCR-5 cell line as well as scintigraphic images of healthy mice after intravenous administration of ^{99m}Tc-DTPA−DIG (PDF)

■ AUTHOR INFORMATION

Corresponding Authors

*E-mail: jennifer.munkert@fau.de (J.M.).

*E-mail: rodrigomaiapadua@ufmg.br. Tel: +55 31 34096946 (R.M.P.).

DOI: 10.1021/acsomega.9b03167
ACS Omega 2019, 4, 22048−22056

ORCID

Jennifer Munkert: 0000-0001-9799-8804

Author Contributions

R.M.P. and A.L.B.d.B. equally designed the study with help of J.M.; R.M.P., A.L.B.d.B, and J.M. conceived and designed the experiments; J.M. and E.R.G. performed the experiments with the help of L.L.M and C.L.M.L.; J.M. R.M.P., and A.L.Bd.B. wrote the paper. B.B.C. isolated the DTPA−DIG. J.D.d.S.F. performed all NMR analyses. All authors interpreted and discussed the data and contributed to the preparation of the final manuscript. The authors further thank Barbara White for linguistic advice.

Notes

The authors declare no competing financial interest.

■ ACKNOWLEDGMENTS

We are very thankful for the financial support of this study by a grant from FFL Stipendiums, FAU (Programm zur Förderung der Chancengleichheit für Frauen in Forschung und Lehre, J.M.), by a grant from the Dr. Hertha and Helmuth Schmauser-Stiftung (J.M.), by a grant from BAYLAT Anschubfinazierung (J.M.), by a grant from EU FP7 IRSES (grant 295251), and by a grant from CNPq (grant 482244/2013-5, R.M.P.) and by a grant from Fapemig (APQ-00538-17, R.M.P.). Further, the authors thank the Brazilian funding agencies CAPES (MEC) and CNPq (MCTI) for their research fellowships as well as CNPq for the financial support.

■ ABBREVIATIONS

^{99m}Tc	technetium-99m
$^{99m}TcO_2$	radiocolloids
$^{99m}TcO_4^-$	pertechnetate
A549	non-small-cell lung cancer
CGs	cardiac glycosides
DIG	digitoxigenin
DMSO	dimethyl sulfoxide
DTPA	diethylenetriaminepentaacetic acid
FBS	fetal bovine serum
MRC-5	human fetal lung fibroblast cell line
MTT	3-(4,5-dimethyl-1,3-thiazole-2-yl)-2,5-diphenyltetrazolium bromide
NSCLC	nonsmall-cell lung cancer
PBS	phosphate-buffered saline
TMS	tetramethylsilane

■ REFERENCES

(1) Siegel, R. L.; Miller, K. D.; Jemal, A. Cancer statistics, 2016. *Ca−Cancer J. Clin.* **2016**, *66*, 7−30.

(2) de Barros, A. L. B.; das Graças Mota, L.; de Aguiar Ferreira, C.; Corrêa, N. C. R.; de Góes, A. M.; Oliveira, M. C.; Cardoso, V. N. 99mTc-labeled bombesin analog for breast cancer identification. *J. Radioanal. Nucl. Chem.* **2013**, *295*, 2083−2090.

(3) Felippe Gonçalves-de-Albuquerque, C.; Ribeiro Silva, A.; Ignácio da Silva, C.; Caire Castro-Faria-Neto, H.; Burth, P. Na/K Pump and Beyond: Na/K-ATPase as a Modulator of Apoptosis and Autophagy. *Molecules* **2017**, *22*, No. 578.

(4) Cherniavsky Lev, M.; Karlish, S. J. D.; Garty, H. Cardiac glycosides induced toxicity in human cells expressing alpha1-, alpha2-, or alpha3-isoforms of Na-K-ATPase. *Am. J. Physiol.: Cell Physiol.* **2015**, *309*, C126−C135.

(5) Clausen, M. V.; Hilbers, F.; Poulsen, H. The Structure and Function of the Na,K-ATPase Isoforms in Health and Disease. *Front. Physiol.* **2017**, *8*, No. 371.

(6) Durlacher, C. T.; Chow, K.; Chen, X.-W.; He, Z.-X.; Zhang, X.; Yang, T.; Zhou, S.-F. Targeting Na(+)/K(+)-translocating adenosine triphosphatase in cancer treatment. *Clin. Exp. Pharmacol. Physiol.* **2015**, *42*, 427−443.

(7) Bertol, J. W.; Rigotto, C.; de Pádua, R. M.; Kreis, W.; Barardi, C. R. M.; Braga, F. C.; Simões, C. M. O. Antiherpes activity of glucoevatromonoside, a cardenolide isolated from a Brazilian cultivar of Digitalis lanata. *Antiviral Res.* **2011**, *92*, 73−80.

(8) Wang, J. K. T.; Portbury, S.; Thomas, M. B.; Barney, S.; Ricca, D. J.; Morris, D. L.; Warner, D. S.; Lo, D. C. Cardiac glycosides provide neuroprotection against ischemic stroke: Discovery by a brain slice-based compound screening platform. *Proc. Natl. Acad. Sci. U.S.A.* **2006**, *103*, 10461−10466.

(9) Elbaz, H. A.; Stueckle, T. A.; Tse, W.; Rojanasakul, Y.; Dinu, C. Z. Digitoxin and its analogs as novel cancer therapeutics. *Exp. Hematol. Oncol.* **2012**, *1*, No. 4.

(10) Calderón-Montaño, J. M.; Burgos-Morón, E.; Orta, M. L.; Maldonado-Navas, D.; García-Domínguez, I.; López-Lázaro, M. Evaluating the cancer therapeutic potential of cardiac glycosides. *BioMed Res. Int.* **2014**, *2014*, No. 794930.

(11) Diederich, M.; Muller, F.; Cerella, C. Cardiac glycosides: From molecular targets to immunogenic cell death. *Biochem. Pharmacol.* **2017**, *125*, 1−11.

(12) Cheung, Y. Y.; Chen, K. C.; Chen, H.; Seng, E. K.; Chu, J. J. H. Antiviral activity of lanatoside C against dengue virus infection. *Antiviral Res.* **2014**, *111*, 93−99.

(13) Ashbrook, A. W.; Lentscher, A. J.; Zamora, P. F.; Silva, L. A.; May, N. A.; Bauer, J. A.; Morrison, T. E.; Dermody, T. S. Antagonism of the Sodium-Potassium ATPase Impairs Chikungunya Virus Infection. *mBio* **2016**, *7*, No. e00693-16.

(14) Gupta, R. S.; Chopra, A.; Stetsko, D. K. Cellular basis for the species differences in sensitivity to cardiac glycosides (digitalis). *J. Cell. Physiol.* **1986**, *127*, 197−206.

(15) Schneider, N. F. Z.; Persich, L.; Rocha, S. C.; Ramos, A. C. P.; Cortes, V. F.; Silva, I. T.; Munkert, J.; Pádua, R. M.; Kreis, W.; Taranto, A. G.; Barbosa, L. A.; Braga, F. C.; Simões, C. M. O. Cytotoxic and cytostatic effects of digitoxigenin monodigitoxoside (DGX) in human lung cancer cells and its link to Na,K-ATPase. *Biomed. Pharmacother.* **2018**, *97*, 684−696.

(16) de Barros, A. L. B.; das Graças Mota, L.; de Aguiar Ferreira, C.; de Oliveira, M. C.; de Góes, A. M.; Cardoso, V. N. Bombesin derivative radiolabeled with technetium-99m as agent for tumor identification. *Bioorg. Med. Chem. Lett.* **2010**, *20*, 6182−6184.

(17) Hanna, A. G.; Elgamal, M. H. A.; Hassan, A. Z.; Duddeck, H.; Simon, A.; Kovács, J.; Tóth, G. Complete1H and13C signal assignments of 5*β*-cardenolides isolated fromAcokanthera spectabilis Hook F. *Magn. Reson. Chem.* **1998**, *36*, 936−942.

(18) de Barros, A. L. B.; das Graças Mota, L.; de Aguiar Ferreira, C.; Cardoso, V. N. Kit formulation for 99mTc-labeling of HYNIC-betaAla-Bombesin(7-14). *Appl. Radiat. Isot.* **2012**, *70*, 2440−2445.

(19) de Barros, A. L. B.; de Oliveira Ferraz, K. S.; Dantas, T. C. S.; Andrade, G. F.; Cardoso, V. N.; de Sousa, E. M. B. Synthesis, characterization, and biodistribution studies of (99m)Tc-labeled SBA-16 mesoporous silica nanoparticles. *Mater. Sci. Eng., C* **2015**, *56*, 181−188.

(20) Zhang, K.; Aruva, M. R.; Shanthly, N.; Cardi, C. A.; Rattan, S.; Patel, C.; Kim, C.; McCue, P. A.; Wickstrom, E.; Thakur, M. L. PET imaging of VPAC1 expression in experimental and spontaneous prostate cancer. *J. Nucl. Med.* **2007**, *49*, 112−121.

(21) Newman, R. A.; Yang, P.; Pawlus, A. D.; Block, K. I. Cardiac glycosides as novel cancer therapeutic agents. *Mol. Interventions* **2008**, *8*, 36−49.

(22) Vedovato, N.; Gadsby, D. C. Route, mechanism, and implications of proton import during Na+/K+ exchange by native Na+/K+-ATPase pumps. *J. Gen. Physiol.* **2014**, *143*, 449−464.

(23) Kaplan, J. H. Biochemistry of Na,K-ATPase. *Annu. Rev. Biochem.* **2002**, *71*, 511−535.

DOI: 10.1021/acsomega.9b03167
ACS Omega 2019, 4, 22048−22056

(24) Schneider, N. F. Z.; Cerella, C.; Simões, C. M. O.; Diederich, M. Anticancer and Immunogenic Properties of Cardiac Glycosides. *Molecules* **2017**, *22*, No. 1932.
(25) Zhang, L.; Zhang, Z.; Guo, H.; Wang, Y. Na+/K+-ATPase-mediated signal transduction and Na+/K+-ATPase regulation. *Fundam. Clin. Pharmacol.* **2008**, *22*, 615−621.
(26) Mijatovic, T.; Roland, I.; van Quaquebeke, E.; Nilsson, B.; Mathieu, A.; van Vynckt, F.; Darro, F.; Blanco, G.; Facchini, V.; Kiss, R. The α1 subunit of the sodium pump could represent a novel target to combat non-small cell lung cancers. *J. Pathol.* **2007**, *212*, 170−179.
(27) Schneider, N. F. Z.; Cerella, C.; Lee, J.-Y.; Mazumder, A.; Kim, K. R.; Carvalho, A.; de Munkert, J.; Pádua, R. M.; Kreis, W.; Kim, K.-W.; Christov, C.; Dicato, M.; Kim, H.-J.; Han, B. W.; Braga, F. C.; Simões, C. M. O.; Diederich, M. Cardiac Glycoside Glucoevatromonoside Induces Cancer Type-Specific Cell Death. *Front. Pharmacol.* **2018**, *9*, No. 70.
(28) Boff, L.; Munkert, J.; Ottoni, F. M.; Zanchett Schneider, N. F.; Ramos, G. S.; Kreis, W.; Fernandes de Andrade, S.; Dias de Souza Filho, J.; Braga, F. C.; Alves, R. J.; Maia de Pádua, R.; Oliveira Simões, C. M. Potential anti-herpes and cytotoxic action of novel semi-synthetic digitoxigenin-derivatives. *Eur. J. Med. Chem.* **2019**, *167*, 546−561.
(29) Espineda, C.; Seligson, D. B.; James Ball, W.; Rao, J.; Palotie, A.; Horvath, S.; Huang, Y.; Shi, T.; Rajasekaran, A. K. Analysis of the Na,K-ATPase α- and β-subunit expression profiles of bladder cancer using tissue microarrays. *Cancer* **2003**, *97*, 1859−1868.
(30) Avila, J.; Lecuona, E.; Morales, M.; Soriano, A.; Alonso, T.; Martín-Vasallo, P. Opposite Expression Pattern of the Human Na, K-ATPase β1 Isoform in Stomach and Colon Adenocarcinomasa. *Ann. N. Y. Acad. Sci.* **1997**, *834*, 653−655.
(31) Lefranc, F.; Mijatovic, T.; Kondo, Y.; Sauvage, S.; Roland, I.; Debeir, O.; Krstic, D.; Vasic, V.; Gailly, P.; Kondo, S.; Blanco, G.; Kiss, R. Targeting the alpha 1 subunit of the sodium pump to combat glioblastoma cells. *Neurosurgery* **2008**, *62*, 211−221 discussion 221-2.
(32) Oda, C. M. R.; Fernandes, R. S.; de Araujo Lopes, S. C.; de Oliveira, M. C.; Cardoso, V. N.; Santos, D. M.; de Castro Pimenta, A. M.; Malachias, A.; Paniago, R.; Townsend, D. M.; Colletti, P. M.; Rubello, D.; Alves, R. J.; de Barros, A. L. B.; Leite, E. A. Synthesis, characterization and radiolabeling of polymeric nano-micelles as a platform for tumor delivering. *Biomed. Pharmacother.* **2017**, *89*, 268−275.
(33) Ujvari, B.; Casewell, N. R.; Sunagar, K.; Arbuckle, K.; Wüster, W.; Lo, N.; O'Meally, D.; Beckmann, C.; King, G. F.; Deplazes, E.; Madsen, T. Widespread convergence in toxin resistance by predictable molecular evolution. *Proc. Natl. Acad. Sci. U.S.A.* **2015**, *112*, 11911−11916.
(34) Berry, R. G.; Despa, S.; Fuller, W.; Bers, D. M.; Shattock, M. J. Differential distribution and regulation of mouse cardiac Na+/K+-ATPase alpha1 and alpha2 subunits in T-tubule and surface sarcolemmal membranes. *Cardiovasc. Res.* **2007**, *73*, 92−100.
(35) Doherty, J. E. The clinical pharmacology of digitalis glycosides: a review. *Am. J. Med. Sci.* **1968**, *255*, 382−414.
(36) Iisalo, E. Clinical Pharmacokinetics of Digoxin. *Clin. Pharmacokinet.* **2012**, *2*, 1−16.
(37) Chatterjee, M.; Ganguly, S.; Sarkar, B. R.; Banerjee, S. Technetium-99m radiolabeled ouabagenin-cysteine conjugate: Biological evaluation in animal models. *Nucl. Med. Biol.* **1996**, *23*, 115−120.
(38) Yoda, A.; Hokin, L. E. On the reversibility of binding of cardiotonic steroids to a partially purified (Na+K)-activated adenosinetriphosphatase from beef brain. *Biochem. Biophys. Res. Commun.* **1970**, *40*, 880−886.
(39) Fujibayashi, Y.; Takemura, Y.; Matsumoto, K.; Wada, K.; Yonekura, Y.; Konishi, J.; Yokoyama, A. High myocardial accumulation of radioiodinated digoxin derivative: a possible Na,K-ATPase imaging agent. *J. Nucl. Med.* **1992**, *33*, 545−549.
(40) Baykov, A. A.; Evtushenko, O. A.; Avaeva, S. M. A malachite green procedure for orthophosphate determination and its use in alkaline phosphatase-based enzyme immunoassay. *Anal. Biochem.* **1988**, *171*, 266−270.

DOI: 10.1021/acsomega.9b03167
ACS Omega 2019, 4, 22048−22056